ORIGINAL PAPER

A Highly Sensitive Solid Substrate Room Temperature Phosphorimetry for Carbaryl Detection Based on its Activating Effect on NaIO$_4$ Oxidizing Fluorescein

Jiaming Liu · Qitong Huang · Zhen-bo Liu · Xiaofeng Lin · Li-Hong Zhang · Chang-Qing Lin · Zhi-Yong Zheng

Abstract Fluorescein (HFin) could emit strong and stable room temperature phosphorescence (RTP) signal on polyamide membrane (PAM) using Pb^{2+} as the ion perturber. Carbaryl could activate effect on NaIO$_4$ oxidating HFin, which caused the RTP signal of the system to quench sharply. The phosphorescence intensity (ΔI_p) of activating system higher 3.3 times (119.4/36.0) than that of non-activating system, and is directly proportional to the content of carbaryl. Thus, an activating solid substrate room temperature phosphorimetry (SSRTP) for carbaryl detection has been established. This sensitive (the limit of quantification (LOQ) was 2.0×10^{-13} g mL^{-1}), selective, simple and rapid method has been applied to determine trace carbaryl in water samples with the results consisting with those obtained by fluorimetry, showing its high accuracy. The apparent activation energy (E) and rate constant (k) of this activating reaction were 20.77 kJ mol^{-1} and 1.85×10^{-4} s^{-1}, respectively. Meanwhile, the mechanism of activating SSRTP for carbaryl detection was also discussed using infrared spectra (IR).

J. Liu (✉) · Q. Huang · X. Lin
College of Chemistry and Environment, Minnan Normal University, Zhangzhou 363000, People's Republic of China
e-mail: zzsyliujiaming@126.com

Q. Huang · L.-H. Zhang · C.-Q. Lin · Z.-Y. Zheng
Department of Food and Biological Engineering, Zhangzhou Institute of Technology, Zhangzhou 363000, People's Republic of China

Z.-b. Liu
Xiamen Third hospital, Xiamen 361100, People's Republic of China

Introduction

The joint actions of carbaryl and nitrite have carcinogenic, teratogenic and mutagenic effects [1]. As a kind of environmental estrogens may also affect the gene expression [2] and tumor generation [3]. The epidemiological investigation found that the rate of chromosomal aberrations of carbaryl exposure is higher than that of control group [4]. Therefore, the study on the methods for carbaryl detection has great significance and application prospect to the early warning and prevention of human diseases.

Literature has reported that carbaryl can react with DNA [5], which has been applied to determine trace carbaryl by ultraviolet spectrometry and fluorimetry. The methods available currently for carbaryl detection mainly focus on thin-layer chromatography [6], gas chromatography [7], solid-phase enzyme-linked immunosorbent assay [8], high-performance liquid chromatography [9], fluorimetry [10, 11], high-performance liquid chromatography-mass spectrometry [12], micellar electrokinetic chromatography [13], fluorescence polarization [14], immunosensor method [15], chemiluminescence method [16], capillary electrophoresis [17], electrochemical analysis [18], molecular imprinted polymers method [19] and surface plasmon resonance method [20]. However, the repeatability of gas chromatography is bad on account of easy decomposition of carbaryl, high-performance liquid chromatography is complicated and time-consuming, and much organic solvent is used in the operation process, resulting in environment pollution and harm to the health of operators. Though detection limit of solid-phase extraction pre-concentration and fluorescence derivatization is low [21], but the process of sample preparation is complex. Comparatively, SSRTP more advantages. RTP has a

larger Stocks' shift than fluorescence. Its detecting wavelength is in the long wavelength region and the long RTP lifetime for time resolved analysis show its significant advantage in the detection of trace substances..

According to the manifestation of the RTP signal from the activating effect of carbaryl on $NaIO_4$ oxidizing HFin, a new detection technology for carbaryl residue analysis in water samples has been first developed. The establishment, application and the mechanism research of the new method, not only effectively promote the research process of SSRTP, but also promote the development of environment analysis..

Experimental

Apparatus and Reagents

Phosphorescent measurements were carried out on a LS-55 luminescence spectrophotometer with a solid surface analysis apparatus (Perkin Element Corporation, U.S.A.). The instrument's main parameters are as follows: delay time 0.1 ms, gate time 2.0 ms, cycle time 20 ms, flash count 1, excitation slit 10 nm, emission slit 15 nm, scan speed 1,500 nm min^{-1}. KQ-250B ultrasonic washing machine (Kunshan Ultrasonic Machine Corporation, China), AE240 electronic analytical balance (Mettler-Toledo Instruments Corporation, China) and a 0.50-μL flat head micro-injector (Shanghai Medical Laser Instrument Plant, China) were used.

Carbaryl (National institute for the control of pharmaceutical and biological products) stock solution: carbaryl was dissolved to $3.0 \times 10-5$ g mL−1 with ethanol as stock solution and put in refrigeratory at 4 °C for use. Then the stock solution was diluted to 100.00, 10.0 and 1.0 p g mL−1 as work solution. $3.0 \times 10-4$ g mL−1 HFin ethanol solution, Preparation of EDC-NHS coupling agent solution: the mixture of 5 mM 1-ethyl-3-3-dimethylaminopropylcarbodiimide hydrochloride (EDC, Alfa Company) and 5 mM N-hydroxysucci-nimide (NHS, Alfa Company) was prepared with 40 % ethanol. 1.0 mol L−1 Pb2+ and 0.015 % $NaIO_4$ solution were also used in the experiment. All reagents were analytical regent grade except for carbaryl was primary standard reagent. The water used was prepared by three times sub-boiling distillation.

Filter paper was purchased from Xinhua Paper Corporation (Hangzhou, China). PAM, acetic acid cellulose membrane (ACM) and nitric acid cellulose membrane (NCM) were purchased from Luqiaosijia biochemical plastic plant (Hangzhou, China). The paper sheets were pre-cut into small wafers (Diameter is 15 mm) and a ring indentation (Diameter is 4.0 mm) at the center of each wafer made by a standard pinhole plotter for use.

Experimental Method

Certain amount of carbaryl, 1.00 mL HFin, 2.00 mL $NaIO_4$ and 1.00 mL EDC-NHS were added into a 25-mL colorimetric tube, mixed homogeneously, and then diluted to 25 mL with water. The colorimetric tube was kept at 100 °C for 10 min. The PAM with a ring indentation (diameter is 4.0 mm) was immersed in 1.00 mol L^{-1} Pb^{2+} solution for 10 s, and dried at 90 ± 1 °C for 2 min. A 0.40 μL drop of test solution and blank solution were suspended onto the center of the PAM, dried at 90 ± 1 °C for 2 min. At the same time, a blank test was also conducted. The phosphorescence intensity of test solution (I_p) and reagent blank (I_{p0}) were directly measured at 480 / 646 nm ($\lambda_{ex}^{max}/\lambda_{em}^{max}$). Then, ΔI_p ($=I_{p0}-I_p$) was calculated.

IR Analysis of HFin-CO-HN-CH$_3$, HFin, HFin', Carbary and Naphthoquinone

100.0 pg carbaryl, 1.00 mL HFin, 2.00 mL $NaIO_4$ and 1.00 mL EDC-NHS were added into a 25-mL colorimetric tube, mixed homogeneously, and then diluted to 25 mL with water. Then, the colorimetric tubes were heated in water bath at 100 °C for 10 min, cooled by flowing water for 5 min. Transferred to separatory funnels, mixture was respectively extracted with 9.00 mL CH_3OH-H_2O (55:45) for three times. The extracts were collected, evaporated, dried in vacuum, finally HFin-CO-HN-CH$_3$ was obtained. To both of two 25-mL colorimetric tubes, 10.00 mL of 3.0×10^{-3} mol L^{-1} HFin and 5.00 mL of 0.015%$NaIO_4$, 10.00 mL of 3.0×10^{-4} g.mL^{-1} carbary were added, respectively, diluted to 25 mL with water and mixed homogeneously. After reacting at 100 °C for 10 min, 5.00 mL mixture was dried at 100 ± 1 °C for 60 min, respectively, straight away HFin' and

Scheme 1 Reaction between $NaIO_4$ and HFin
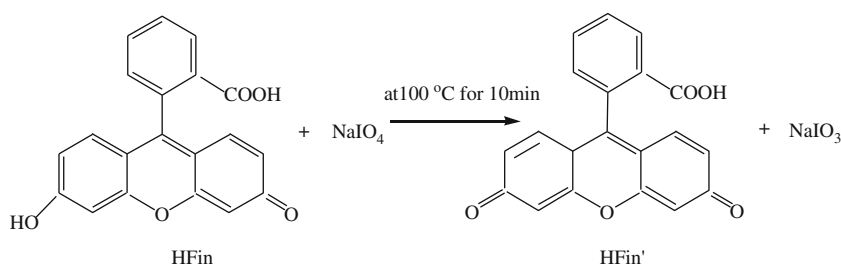
Table 1 Infrared spectra data of HFin″ (HFin'-CO-HN-CH₃), HFin, HFin', Carbary and Naphthoquinone' (ν is stretching vibration; δ is in-plane bending vibration and w is out-plane bending vibration)

Sample	−OH (cm⁻¹)	−C=O (cm⁻¹)	−C₆H₅ (cm⁻¹)	Phenazine ring C=C (cm⁻¹)	Naphthol ring C=C (cm⁻¹)	−H−N− (cm⁻¹)	−NH₂ (cm⁻¹)	−CH₃ (cm⁻¹)
HFin	ν: 3345.6	ν: 1736.3	ν: 1609.1 ν: 1494.3 ν: 1440.9	ν: 1612.7 ν: 1533.4				
HFin'		ν: 1738.5	ν: 1611.2 ν: 1495.6 ν: 1441.8	ν: 1613.5 ν: 1534.8				
H₂NCH₃							ν: 3481.3	ν: 2960.7 ν: 2858.4 ν: 1463.5
HFin″ (HFin'-CO-HN-CH₃)		ν: 1714.9	ν: 1609.7 ν: 1493.2 ν: 1438.4	ν: 1610.7 ν: 1531.4		ν: 1545.7		ν: 2958.3 ν: 2856.8 ν: 1462.2
Carbary		ν: 1712.7 δ: 1101.5			ν: 1614.3 δ:1535.9	ν: 3452.4 δ: 1495.6		ν: 2962.2 ν:2870.8 ν:1464.7
Naphthoquinone		ν: 1713.4 δ: 1102.1			ν:1615.7 δ:1536.4			

naphthoquinone were obtained. Infrared spectra of HFin-CO-HN-CH₃, HFin, HFin', carbary and naphthoquinone HFin-CO-HN-CH₃, HFin, HFin', carbary and naphthoquinone were scanned after the sample preparation by pressed disc method with KBr, respectively.

Results and Discussion

Mechanism of the Reaction

HFin could emit strong and stable RTP signal on PAM when Pb^{2+} was used as the ion perturber. The $NaIO_4$ was similar to Cu^{2+} [22], it could oxidate HFin to form a non-phosphorescent compound (HFin') at 100 °C for 10 min, which lead the RTP of the system to quench. The reaction is shown in Scheme 1.

In order to prove the possibility of oxidizing reaction between $NaIO_4$ and HFin to form the HFin', the structure of HFin and HFin' were analyzed with IR, respectively, and the results are listed in Table 1. The IR of HFin' kept the most characteristic adsorption peak of HFin, but the intensity of stretching vibration peak for −OH (ν: 33345.6 cm⁻¹) disappeared, while the intensity of stretching vibration peak for −C=O (ν: 1738.5 cm⁻¹) enhanced greatly. Thus, it could conclude that the −OH of HFin was oxidized to form the −C=O.

In the presence of carbaryl, carbaryl was hydrolyzed to form the naphthol, H_2NCH_3 and CO_2, while naphthol was oxidized to form the naphthoquinone (Scheme 2) [10].

The IR of naphthoquinone kept the characteristic adsorption peak of naphthol ring from carbary, but the stretching vibration peak of −H−N for carbary at ν3452.4 cm⁻¹ and δ 1495.6 cm⁻¹, −CH₃ for carbary at ν2870.8 cm⁻¹ and δ1464.7 cm⁻¹ disappeared, while the intensity of stretching vibration peak for −C=O (ν: 1713.4 cm⁻¹) enhanced greatly. These facts above confirmed the probability of the carbaryl hydrolyzed to form the naphthoquinone.

The formed H_2NCH_3 was similar to concanavalin A [23], EDC firstly coupled with the –COOH of HFin' to form HFin'-COO-EDC, which reacted with NHS to generate HFin'-COO-NHS [24], and at last HFin'-COO-NHS reacted with the −NH₂ of H_2NCH_3 to produce the product HFin″(HFin-CO-HN-CH₃, Scheme 3) [25]. The negative induction effect was produced due to the higher electronegativity of N atom than that of C atom in HFin-CO-HN-CH₃, which resulted in the π electron density in the HFin conjugated system to decrease, causing the RTP of the system to quench.

Seen from IR, stretch vibration absorption peak of –NH₂ group in H_2NCH_3 located at 3481.3 cm⁻¹, while stretch vibration absorption peak of –CH₃ group in H_2NCH_3 located at 2960.7 cm⁻¹, 2858.4 cm⁻¹ and 1463.5 cm⁻¹, the infrared spectra of HFin″ kept the most characteristic adsorption peak of HFin'and H_2NCH_3, but the stretching vibration peak of –

Scheme 2 Hydrolysis of carbaryl
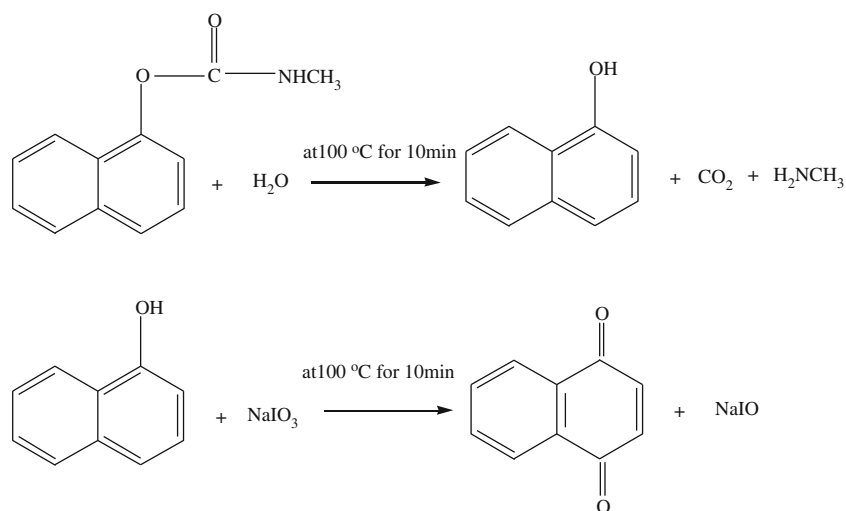
NH$_2$ group for H$_2$NCH$_3$ at 3481.3 cm^{-1} disappeared and the stretching vibration peak of C=O group blue shift from 738.5 to 1714.9 cm^{-1}, the stretching vibration peak of −H−N− group appeared at 1545.7 cm^{-1}, indicating the formation of –CO–NH– bond. The changes of these peaks fully demonstrated the possibility of H$_2$NCH$_3$ reacted with HFin' to generate HFin'-CO-HN-CH$_3$.

In the reaction progress, carbaryl accelerated the oxidation reaction between NaIO$_4$ and HFin, causing the RTP of HFin to sharply quench.. Compared with the oxidation reaction between NaIO$_4$ and HFin, carbaryl showed stronger activating effect and its ΔI_p is 6.5 times than that of non-activating reaction. Thus, activating SSRTP method could be used to determine trace carbaryl.

In order further to prove the probability of activating reaction mechanism of NaIO$_4$ oxidizing HFin by carbaryl, the E and k were investigated under the optimal condition above. For the system containing 0.48 fg spot^{-1}, 1/T×1000 was positive

Scheme 3 Reaction between H$_2$NCH$_3$ and HFin
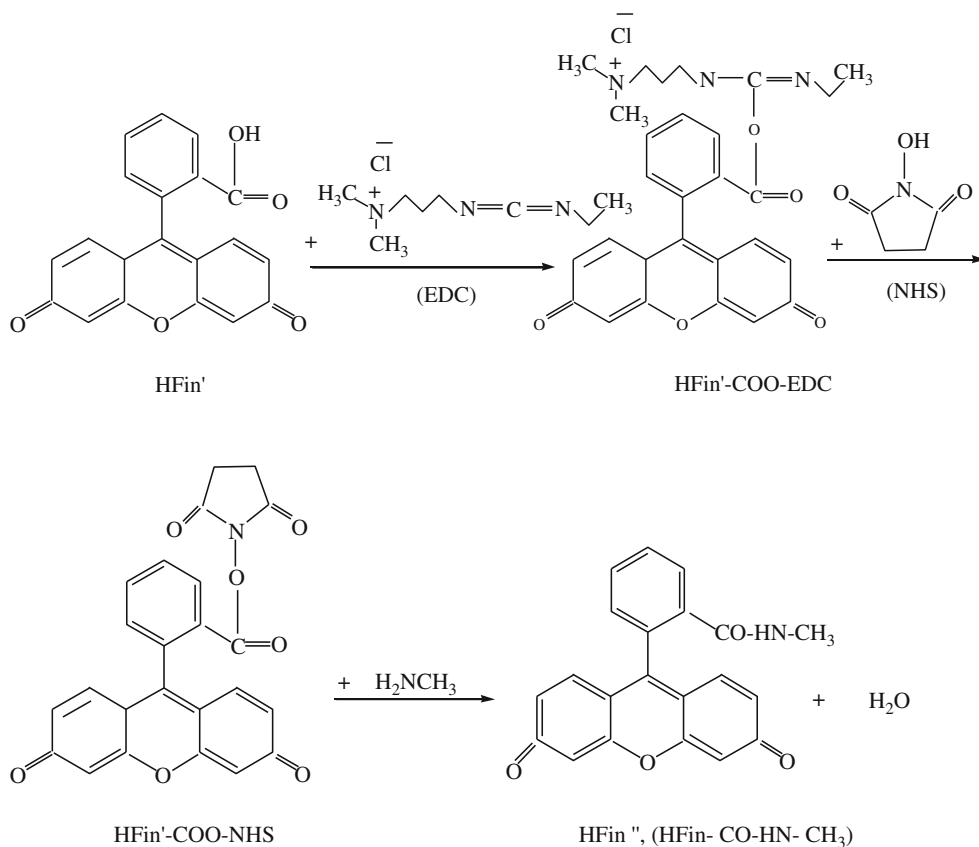
Fig. 1 Phosphorescence spectra of carbary1-NaIO$_4$-HFin system (Curves 1–6 are excitation spectra, curves 1′–6′ are emission spectra.)
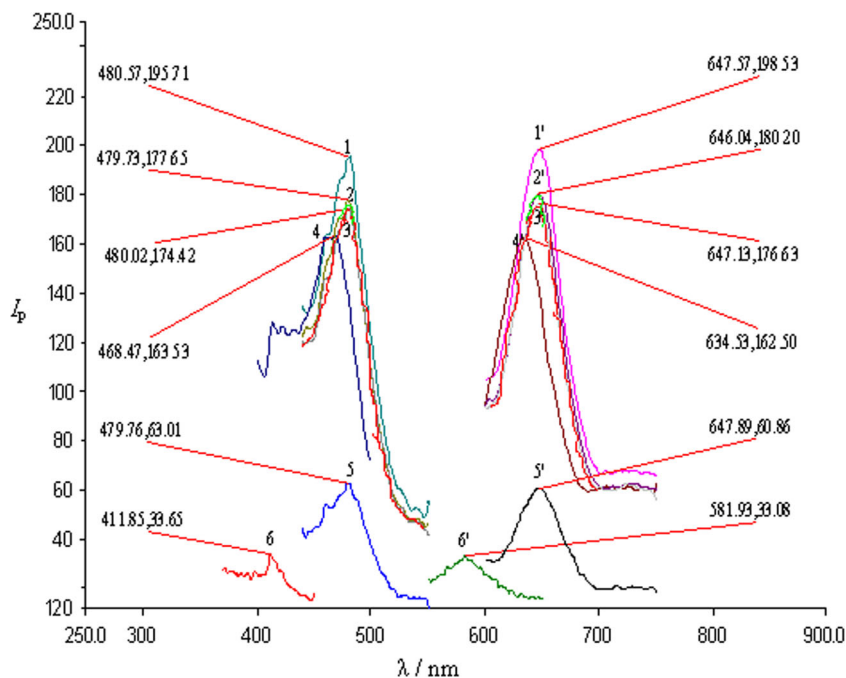
correlated with—log [log I_{p0}/I_p] in the range of 35–100 °C. The regression equation was—log [log I_{p0}/I_p]=0.9319×(1/T)×1000+1.5492, r=0.9994. Time was positive correlated with ln I_{p0}/I_p in the range of 2–10 min. The regression equation was ln I_{p0}/I_p=−0.012+0.013 t (min), r=0.9912. When the temperature and time were 100 °C and 10 min, the E and k were 20.77 kJ mol^{-1} and 1.85×10^{-4} s^{-1}, respectively. E and k have proved that carbaryl had an activate effect on the reaction of NaIO$_4$ oxidizing HFin, and the activation reaction was the first grade. These facts above not only confirmed the activating effect of carbaryl on oxidation reaction between NaIO$_4$ and HFin, but also demonstrated the probability of reaction mechanism for carbaryl detection.

Excitation Spectra and Emission Spectra

The RTP spectra of carbary1-NaIO$_4$-HFin system was shown in Fig. 1 and Table 2. Results indicate that HFin could emit strong and stable RTP on the PAM (λ_{ex}^{max} / λ_{em}^{max}=480.4 / 647.6 nm, I_p=198.5, curve 1.1′) with Pb^{2+} as perturber. HFin could be oxidized by NaIO$_4$ to lead to the quenching of RTP (λ_{ex}^{max} / λ_{em}

^{max}=479.7 / 646.0 nm, I_p=180.2, curve 2.2′). The carbary1 also will lead the RTP signal of HFin to quench (λ_{ex}^{max} / λ_{em}^{max}= 468.5 / 634.5 nm, I_p=162.5, curve 4.4′) with λ_{em}^{max} blue shifting for 13.1 nm, which indicated the formation of new compound. When 100.0 pg carbary1 was added in HFin-NaIO$_4$ system, RTP of HFin was quenched sharply (λ_{ex}^{max} / λ_{em}^{max}=479.8 / 648.0 nm, I_p=60.9, ΔI_p=119.4, curve 5.5′). This indicates that carbary1 has strongly activating effect on NaIO$_4$ oxidizing HFin. Furthermore, the content of carbary1 was linear with ΔI_p. Thus, the content of carbary1 could be detected at 480 / 646 nm. The Fig. 1S and Fig. 2S were showed that the λ_{em}^{max} of carbaryl was 472.1 nm, the corresponding fluorescence intensity was 985.3, the λ^{max} of ultraviolet absorption spectrum of carbaryl was 263.4 nm, which indicating that no fluorescence interference at 480 nm (λ_{em}^{max}).

Optimum Measurement Condition for RTP

For the system containing 0.48 fg spot^{-1} carbaryl, the effects of the concentration and dosage of reagents, solid substrates, the species and concentrations of ion perturber, reaction time

Table 2 Phosphorescence characteristics of carbary1-NaIO$_4$-HFin system

System	λ_{ex}^{max} (nm)	λ_{em}^{max} (nm)	I_p	RSD (%)	ΔI_p
1.1′1.00 mL HFin	480.4	647.5	198.5	1.1	
2.2′ 1.1′+2.00 mL NaIO$_4$	479.9	646.0	180.2	1.3	
3.3′ 2.2′+5.0 pg carbaryl	479.9	647.0	176.6	1.6	3.6
4.4′1.1′+100.0 pg carbaryl	468.6	634.4	162.5	1.9	36.0
5.5′ 2.2′+100.0 pg carbaryl	478.0	648.1	60.8	2.1	119.4
6.6′ PAM	412.0	582.0	33.1	3.6.	

Table 3 Optimization of the various parameters

Measurement conditions	Parameters	The ΔI_p in carbary1-NaIO$_4$-HFin. system	Optimal
HFin (1.0×10^{-4} mol·L^{-1})	0.050, 0.10, 0.20, 0.30, 0.40	22.9, 32.1, 40.6, 38.2, 33.9	3.0×10^{-4} mol L^{-1}
RSDs (%)		4.0, 3.6, 3.0, 3.2, 3.4	
HFin (mL)	0.10, 0.50, 1.00, 1.50, 2.00	19.6, 31.8, 40.4, 37.0, 34.8	1.00 mL
RSDs (%)		4.2, 3.7, 2.8, 3.3, 3.1	
NaIO$_4$ (%)	0.0050, 0.010, 0.015, 0.020, 0.025	33.1, 36.2, 40.3, 36.9, 34.7	0.015 %
RSDs (%)		3.6, 3.3, 3.1, 3.4, 3.5	
NaIO$_4$ (mL)	0.50, 1.00, 1.50, 2.00, 2.50	23.3, 30.2, 38.0, 40.6, 38.7	2.00 mL
RSDs (%)		3.9, 3.6, 3.4, 0.3.2, 3.5	
C $_{Pb}^{2+}$ (mol L^{-1})	0.10, 0.50, 1.00, 1.50, 2.00	25.2, 30.0, 40.4,35.8, 34.3	1.00 mol L^{-1}
RSDs (%)		3.8, 3.5, 3.1, 3.3, 3.3	
Oxidant	K$_2$S$_2$O$_8$, KClO$_3$, (NH$_4$)$_2$S$_2$O$_8$, NaIO$_4$, H$_2$O$_2$	17.5, 23.3, 40.8, 31.6, 26.9	NaIO$_4$
RSDs (%)		4.6, 3.8, 3.0, 3.4, 3.7	
Solid substrate	PAM, ACM, NCM, Paper	40.1, 18.7, 23.8, 33.1	PAM
RSDs (%)		2.9, 4.5, 3.7, 3.4	
Ion perturber	I$^-$, Hg^{2+},A g$^+$, Pb^{2+}	14.6, 26.1, 31.6, 40.4	Pb^{2+}
RSDs (%)		4.5, 3.6, 3.3, 3.0	
Reaction time (min)	2, 4, 6, 8,10,12	10.3, 15.5, 21.4, 30.6, 40.8, 37.4	10 min
RSDs (%)		4.6, 4.4, 3.8, 3.5, 2.9, 3.1	
Reaction temperature (°C)	35, 55, 65, 85, 100	13.3, 20.0, 23.9, 34.0, 40.4	100 °C
RSDs (%)		4.4, 3.6, 3.4, 3.2, 2.8	
pH of the reaction	4.60, 5.30, 6.40, 7.50, 8.70	31.5, 39.5, 40.7, 35.4, 27.1	6.40
RSDs (%)		3.4, 3.0, 2.7, 3.2, 3.5	
Passing drying N$_2$ (min)	3, 6, 10, 15, 20, 25	40.0, 40.8, 40.2, 40.0, 40.7, 40.3	6 min
RSDs (%)		3.0, 2.8, 3.3, 2.9, 3.2, 3.1	
Not passing drying N$_2$ (min)	3, 6,1 0,15, 20, 25	40.7, 38.8, 34.2, 30.0, 27.7, 24.3	
RSDs (%)		2.8, 3.2, 3.4, 3.7, 3.9, 4.0	
Stability of the system (min)	5, 20, 30, 40, 50, 60	40.0, 40.2, 40 0.5, 40.5, 40.6, 33.4	5–50 min
RSDs (%)		3.0, 2.8, 3.1, 2.9, 2.7, 3.2	

Table 4 Effect of coexistent ions or substances

	This method			Ref. [10]
Coexistent ions or substances	Maximum concentration (μg·mL^{-1})	Allowed multiple	Er (%)	Allowed multiple
K$^+$	1.8	1.5×10^6	−4.7	5.0×10^5
Na$^+$	2.4	2.0×10^6	−2.6	5.0×10^5
NH$_4^+$	0.096	8.0×10^4	1.8	2.0×10^4
Al^{3+}	0.036	3.0×10^4	3.5	1.0×10^4
Mg^{2+}	3.6×10^{-3}	3000	−4.3	1000
Fe^{3+}	3.0×10^{-4}	250	−1.4	50
Ca^{2+}	6.0	5.0×10^5	1.2	1.0×10^5
NO$_3^-$	3.6×10^{-3}	3000	2.3	1000
Glucose	6.0	5.0×10^6	4.1	5 0.0×10^5
Ethyl acetate	4.8	4.0×10^6	4.9	5 0.0×10^5
Sodium carboxymethyl cellulose	0.012	10^4	−3.7	1000
Isoprocarb	6.0×10^{-5}	50	−2.4	10
Phloroglucinol	2.5×10^{-4}	210	−1.3	30
Naphthol	2.5×10^{-4}	210	2.4	60
H$_2$NCH$_3$	14.4×10^{-5}	120	3.6	20
Earbosulfan	0.048	400	3.2	80
Gum arabic	0.019	16000	2.1	2000
Fenobucarb	7.2×10^{-5}	60	4.1	10

Table 5 Results of carbaryl in water samples

Sample	SSRTP ($n=6$)						Fluorimetry [10] ($n=5$)	
	Found ($\mu g \cdot mL^{-1}$)	Adding amount ($\mu g \cdot mL^{-1}$)	Recovery ($\mu g \cdot mL^{-1}$)	Obtained ($\mu g \cdot mL^{-1}$)	Recovery (%)	RSD (%)	Found	Er (%)
Rain water	4.21	0.40	4.58	0.37	92.5	4.5	4.24	−0.70
Tap water	5.63	0.60	6.22	0.57	95.0	4.3	5.68	−0.88
Jiulong river water	6.34	0.60	6.92	0.58	96.7	3.8	6.39	−0.78
Lake water	8.95	0.90	9.85	0.90	100.0	3.4	8.91	0.45
Pond water	9.27	0.90	10.18	0.91	101.1	3.0	9.23	0.43

and temperature, reaction acid, oxygen and humidity on the ΔI_p and RSDs (%) of the system were tested in a univariate approach, respectively (Table 3).

From Table 3, we could conclude the following rules:

1. With the increasing of the concentration and dosage of HFin, the ΔI_p of the system enhanced gradually. When the concentration and dosage of HFin was 3.00 mL of 1.0×10^{-4} mol L^{-1}, the ΔI_p of the system reached the maximum, the reason might be that the yield of product HFin-CO-HN-CH$_3$ reached the highest.

2. Though the ΔI_p of the system were high when $K_2S_2O_8$, $KClO_3$, $(NH_4)_2S_2O_8$ and H_2O_2 were chosen as oxidants, they were still lower than that of $NaIO_4$ due to the strongest oxidability of $NaIO_4$ Further investigations found that the ΔI_p of the system enhanced with the increasing of the concentration and dosage of $NaIO_4$ the ΔI_p of the system gradually enhanced. When the concentration and dosage of $NaIO_4$ was 2.00 mL of 0.015 %, the ΔI_p of the system almost stayed invariable.

3. Among the three different solid substrates examined in this study, compared with paper, NCM and ACM, PAM exhibited the highest phosphorescence signal for the reason that the heavy atom Pb^{2+} solution diffused slowly on PAM, but spread rapidly when the PAM was dried [26].

4. Though the ΔI_p of the system were high when I^-, Hg^{2+} and Ag^+ were chosen as ion perturbers, they were still lower than that of Pb^{2+}, which might be that the transition probability from the singlet state (S_1) to triplet state (T_1) of

the luminescence molecule. Further investigations found that the ΔI_p of the system enhanced with the increasing of concentration of Pb^{2+} and reached the maximum when 1.0 mol L^{-1} Pb^{2+} was used. Henceforth, with the further increasing of concentration of Pb^{2+}, the ΔI_p of the system decreased. The reason might be that appropriate heavy atom could increase the intersystem crossing of HFin from S_1 to T_1, which enhanced the RTP signal, while the excessive heavy atom will lead the RTP signal to quench [27].

5. The ΔI_p of the system linearly enhanced with the increasing of pH in the range of 4.60–6.40, while it reached the maximum and remained stable when the pH was 6.40. The reason might be that the activating reaction rate of carbaryl reached the maximum, and the yield of product HFin-CO-HN-CH$_3$ reached the highest.

6. As the reaction time and temperature increased the ΔI_p of the system gradually enhanced, which might result from increasing of the activating ability of carbaryl gradually. When the reaction temperature and time were 100 °C and 10 min, respectively, the ΔI_p of the system reached the maximum, which might be that the activating ability of carbaryl reached the peak.

7. In this experiment, the ΔI_p of the system almost stayed invariable when drying N_2 was passed for 3–25 min. The reason might be that the effect of oxygen and humidity on the RTP was eliminated. However, as the time increasing without passing drying N_2, the ΔI_p of the system decreased, showing the quenching effect of oxygen and

Table 6 Analysis of the significant differences for determination results ($P=90$ %, $f=n_1+n_2-2=9$, $F_{0.90, 9}=6.3$, $t_{0.90, 9}=1.8$)

Sample	SSRTP ($\mu g\ mL^{-1}$) ($n=6$)		Fluorimetry ($\mu g\ mL^{-1}$) ($n=5$)		Statistical analysis		
	$\overline{X}_1$	S_1	$\overline{X}_2$	S_2	F	S	t
Rain water	4.21	0.0576	4.24	0.0476	1.5	0.053	1.0
Tap water	5.63	0.0410	5.68	0.0517	0.60	0.046	1.7
Jiulong river water	6.34	0.0548	6.39	0.0610	0.80	0.058	1.4
Lake water	8.95	0.0410	8.91	0.0517	0.60	0.046	1.5
Pond water	9.27	0.0322	9.23	0.0610	0.30	0.047	1.5

humidity on the RTP. Thus, the time of passing drying N_2 was 6 min.

8. The stability of RTP was the key to determine trace carbaryl by activating SSRTP. Under the optimal conditions mentioned above, the ΔI_p of the system almost stayed invariable and had good repeatability within 5–50 min. But the ΔI_p of the system declined gradually when the standing time was over 50 min, possibly due to the deliquescence of HFin.

Working Curve, Linearity Rang, Detection Limit and Precision

Results show that the ΔI_p of the system had linear relationship with the content of carbaryl within 0.080–1.60 (fg spot^{-1}) under the optimum conditions. The regression equation of working curve was $\Delta I_p = -1.633 + 6.580\ m_{carbaryl}$ (fg spot^{-1}) with the correlation coefficient (r) of 0.9994 ($n=6$). When reagent blank was detected in parallel for 11 times, the standard deviation (Sb) was 0.067. Calculated by 10Sb/k or 3Sb/k (Sb/k refers to the quotient between triple of the blank reagent's standard deviation and the slope of the working curve), the LOQ or the limit of detection (LOD) of this method was 0.10 fg carbaryl spot^{-1} (sample volume: 0.40 μL spot^{-1}, corresponding concentration was 2.0×10^{-13} g mL^{-1}) and 0.031 fg carbaryl spot^{-1} (corresponding concentration was 7.8×10^{-14} g mL^{-1}), respectively. LOD of SSRTP.was 1.3×10^4 times lower than that of fluorimetry (LOD=1.0×10^{-9} g L^{-1}) [10] due to the following possible reasons: firstly, activating reaction of carbary had an amplification effect on measure signal, secondly, the perturbation effect of an external heavy atom (Pb^{2+}) improves the molecule transition rate of HFin from S_1 to T_1, causing the ΔI_p of the system to sharply enhance. The obtained relative standard deviation (RSD.) was 4.8 % for 0.080 fg spot^{-1} and 2.1 % for 1.6 fg spot^{-1} carbary, respectively ($n=6$), demonstrating an excellent precision of the SSRTP. This method not only offers a new technology for carbaryl detection, but also shows that amplification effect on measure signal of activating reaction is an effective way to futher improve the sensitivity of SSRTP.

Interference Test

To assess the selectivity of the SSRTP, the effects of foreign ions (substances) on the carbaryl detection were investigated. The interfering effect is defined as the concentration of interfering ions (substances) that can change the probe toward carbary1, when the relative error was more than ±5 %. In the detection process, 1.2 pg carbary1. mL^{-1} was added to each sample and the other interferential ions (substances) were added subsequently, and the results are listed in Table 4.

As shown in Table 4, the allowed multiple of coexistent ions (substances) of this SSRTP were larger than those in Ref.

[10], showing that coexistent ions (substances) have little interference to carbaryl detection and that this SSRTP has good selectivity. The main reason might be that the activating reaction had high selectivity.

Sample Analysis

In order to study the potential applicability of the SSRTP, took 1.00 mL rain water, tap water, Jiulong river water, lake water and pond water, and diluted to 1.0×10^5 multiples respectively, and carbaryl detection in 1.00 ml real samples solution was performed according to the described procedures in Section 2.2. Besides, the standard recovery experiment was also carried out. The results had been compared with those obtained by fluorimetry [10] and listed in Table 5. The significant difference analysis between the designed SSRTP and fluorimetry for carbaryl detection was shown in Table 6.

As was shown in Table 5, this SSRTP has been applied to carbaryl detection in the water samples and the results agreed well with fluorimetry, and RSD was lower than 5 %, which showed that the SSRTP has good accuracy and precision.

Seen from Table 6, the F was 1.5, 0.6, 0.80, 0.60 and 0.30 for the water samples, respectively, indicating that there was no significant differences between S_1 and S_2, and the corresponding t was 1.0,1.7, 1.4, 1.5 and 1.5, respectively, indicating that there was also no significant differences between $\overline{X}_1$ and $\overline{X}_2$. Obviously, the results obtained by the proposed SSRTP were tallied well with those obtained by fluorimetry, indicating that the designed SSRTP was sensitive and accurate and was suitable for carbaryl detection in water samples.

Conclusion

This new SSRTP of carbaryl activating $NaIO_4$ oxidizing HFin to determine trace carbaryl had good sensitivity and selectivity, which was suitable for carbaryl detection in environmental waters. The RTP amplification effect of activating reaction not only proposed a new path for increasing the sensitivity of SSRTP, but also promoted the research process of the residue analysis of trace carbaryl.

References

1. Kanan MC, Kanan SM, Patterson HH (2003) Luminescence properties of silver(I)-exchanged zeolite Y and its use as a catalyst to photodecompose carbaryl in the presence of natural organic matter. Res Chem Intermed 29:691–704

2. Kavlock RJ, Daston GP, DeRosa C, Fenner-Crisp P, Gray LE, Kaattari S, Lucier G, Luster M, Mac MJ, Maczka C, Miller R, Moore J, Rolland R, Scott G, Sheehan DM, Sinks T, Tilson HA (1996) Research needs for the risk assessment of health and environmental effects of endocrine disruptors: a report of the U. S. EPA-sponsored workshop. Environ Health Perspect 104:715–740

3. Lin CC, Hui MN, Cheng SH (2007) Toxicity and cardiac effects of carbaryl in early developing zebrafish (Danio rerio) embryos. Toxicol Appl Pharmacol 222:159–168

4. Sonnenschein C, Soto AM (1998) An updated review of environmental estrogen and androgen mimics and antagonists. J Steroid Biochem 65:143–150

5. Shih I, Van Y (2001) The production of poly-(γ-glutamic acid) from microorganisms and its various applications. Bioresour Technol 79: 207–225

6. Rane KD, Mali BD, Garad MV (1997) Thin-layer chromatographic detection of CarbamateInsecticides using zine (II)Hexacyanoferrate (III) as spray reagent. Chromatogr Mod TLC 10:220–222

7. Forlanl F (1992) Development of enzyme linked immunosorbent assay for triazole fungicides. J Agric Food Chem 40:328–331

8. Abad A, Moreno MJ, Pelegrí R, Martínez MI, Sáez A, Gamón M, Montoya A (2001) Monoclonal enzyme immunoassay for the analysis of carbaryl in fruits and vegetables without sample cleanup. J Agric Food Chem 49:1707–1712

9. Li HP, Li JH, Li GC, Jen J (2004) Simultaneous determination of airborne carbamates in workplace by high performance liquid chromatography with fluorescence detection. Talanta 63:547–553

10. Du YS, Chen GH, Hou FF, Cao J (2006) Fluorescent Spectrophotometric determination of hydrolytic residue carbaryl sensitized by cetyltrimethylammonium bromide fluorescent spectrophotometric determination of hydrolytic residue carbaryl sensitized by cetyltrimethylammonium bromide. Chin J Anal Chem 2006(34): 521–524

11. Jia G, Li L, Qiu J, Wang X, Zhu W, Sum Y, Zhou Z (2007) Determination of carbaryl and its metabolite 1-Naphthol in water samples by fluorescence spectrophotometer after anionic surfactant micelle-mediated extraction with sodium dodecylsulfate. Spectrochim Acta A 67:460–464

12. Granby K, Andersen JH, Christensen HB (2004) Analysis of pesticides in fruit, vegetables and cereals using methanolic extraction and detection by liquid chromatography-tandem mass spectrometry. Analy Chim Acta 520:165–176

13. Lidia MP, Javier HB, Teresa MM (2008) Pesticide analysis in tomatoes by solid-phase microextraction and micellar electrokinetic chromatography. J Chromatogr A 1185:151–154

14. Sánchez FG, Dıaz AN, Torijas MC (2000) Selective determination of carbaryl and benomyl by fluorescence polarization. Anal Chim Acta 414:25–32

15. Mauriz E, Calle A, Abad A, Montoya A, Hildebrandt A, Barceló D, Lechuga LM (2006) Determinationof carbaryl in natural water samples by a surface plasmon resonance flow-through immunosensor. Biosens Bioelectron 21:2129–2136

16. Pulgarín JAM, Molina AA, López PF (2006) Automatic chemiluminescence-based determination of carbaryl in various types of matrices. Talanta 68:586–593

17. Simpson SL Jr, Quirino JP, Terabe S (2008) On-line sample preconcentration in capillary electrophoresis: fundamentals and applications. J Chromatogr A 1184:504–554

18. Miwa DW, Malpass GRP, Machado SAS (2006) Electrochemical degradation of carbaryl on oxide electrodes Water Research, 40: 3281–3289

19. Israel SB, Kal K, José MCF (2007) A molecularly imprinted polymer for carbaryl determination in water. Sensors Actuators B Chem 123: 798–804

20. Mauriz E, Calle A, Abad A (2006) Determination of carbaryl in natural water samples by a surface plasmon resonance flow-through immunosensor. Biosens Bioelectron 21:2129–2136

21. Morrica P, Fidente P, Seccia S (2005) Liquid chromatographic determination of nine N-methylcarbamates in drinking water. Biomed Chromatogr 19:107–110

22. Chen GH, Huang CS (1988) A study of the chemiluminescence of some acidictriphenylmethane dyes. Talanta 35:625–631

23. Liu JM, Xu LY, Hu SR, Wei L, Yang TL, Zhu GH, Huang XM, Li ZM, Chen XH (2008) Determination of glucose by affinity adsorption solid substrate-room temperature phosphorimetry based on concanavalin agglutinin labeled with fluorescein using 1.5-generation dendrimers as sensitizer. Microchim Acta 161:217–224

24. Mi L, Wu K, Gao JY, Li SW, Xi YH, Zhang S (2008) Study on determination of bovine serum albumin by fluorescence resonance energy transfer. Chem Res Appl 20:181–183

25. Angele P, Abke J, Kujat R, Faltermeier H, Schumann D, Nerlich M, Kinnera B, Englerta C, Ruszczakc R, Mueller R (2004) Influence of different collagen species on physico-chemical properties of crosslinked collagen matrices. Biomaterials 25:2831–2841

26. Zhu RH, Jin WJ (2006) Principle and application of room temperature phosphorescence. Scientific Press, Beijing, p 25

27. Liu JM, Lin LP, Wang XX, Cai WL, Zhang LH, Lin SQ (2012) A highly sensitive coupling technique for the determination of trace quercetin based on solid substrate room temperature phosphorimetry and poly (vinyl alcohol) complex imprinting. Anal Chim Acta 723: 76–82